Registration of Range Measurements With Compact Surface Representation

Pierre Payeur, *Member, IEEE,* and Changzhong Chen

***Abstract*—This paper introduces an automatic approach for the estimation of registration parameters between successive viewpoints visited by a laser range sensor. The proposed technique works directly on the raw range measurements and does not require any external device for pose estimation nor any sophisticated feature extraction or triangular mesh computation. Assuming only object rigidity and some overlap between the scanned areas, the approach allows to estimate the full set of six parameters that define geometrical transformations in three-dimensional space. A compact modified Gauss sphere representation is used to encode a simple planar patch approximation of the objects' surface and to validate mapping between the measurements collected from different viewpoints. The technique also makes use of the compact surface representation to successively estimate the rotation and the translation parameters between sensor viewpoints. This solution results in an important reduction of the computational workload and provides sufficient accuracy for most robot navigation applications. The proposed approach performances are demonstrated in an experimental context using real range measurements collected from a series of viewpoints.**

***Index Terms*—Data registration, pose estimation, range measurements, surface segmentation, three-dimensional (3-D) modeling.**

I. Introduction

BUILDING virtual representations of large three-dimensional (3-D) objects or environments from range measurements requires that data are gathered from many different viewpoints. This requirement results from the complexity of objects to be modeled, from the limited field of view of sensors and from occlusions that occur between objects. Each dataset gathered from a given point of view is defined with respect to a local sensor-based reference frame. As a result, the sensor position and orientation at each viewpoint must be estimated to ensure that the information obtained from all sources is merged in a consistent way to build a reliable 3-D model. The problem of registration consists of determining the geometric relationships that exist between these different views provided by the sensor.

The sensor pose can be measured with external means such as magnetic position and orientation trackers, robotic arms, or even CCD cameras providing images from which the sensor position and orientation can be extracted. The latter solution implies very complex image processing and pattern recognition algorithms that are time consuming and rarely fully reliable. The first two approaches appear to be more realistic. A magnetic position and orientation tracking device has been tested in our robotic workcell. Unfortunately, these devices appear to be mainly dedicated to human body tracking as the magnetic fields they use are very sensitive to metallic parts that are commonly found in a robotic setup. On the other hand, when a robotic arm is used to move the sensor from one viewpoint to another, the internal encoders of the robot also provide a good estimate of the sensor position and orientation. However, the sensor is then constrained to the robot physical workspace and cannot get an access to narrow areas of the environment. In many applications, such an approach might reveal to be very limitative. Some specific approaches using external positioning strategies can be found in the literature: Miller [1] uses an autonomous helicopter with a differential global navigation system to build terrain models. Normand [2] uses multiple sonar sensors rigidly mounted on a mobile platform to construct indoor-3-D representations for autonomous robot navigation. Others examples using precalibrated devices or manual assistance can also be found in [3]–[5].

An interesting solution to estimate range sensor registration between successive viewpoints without any peripheral devices is to take advantage of the raw range data provided by the sensor. Assuming that there is a sufficient overlap between the areas of the scene that are measured from each viewpoint, it becomes possible to search for some matching characteristics in both sets of information and then to compute the necessary registration information that makes the projections of those matching elements to superpose after transformation.

In spite of the fact that the registration problem between range measurements has been studied for a while in computer vision, no extensive and definitive solution has been found yet. Many variations to the widely known iterative closest point (ICP) algorithm [6] have been proposed to match characteristic point sets [7]–[10], curves, meshes [11], [12] or parametric surfaces [13], [14]. Some approaches use both range and intensity data, also provided by most range sensors, to improve their selection of control points that are to be matched [15], [16]. These algorithms generally provide good results but the search for characteristic curves or surfaces is very complex and time consuming.

Moreover, research works on the topic of registration generally assume that full range images are directly available from the sensors [17]. Such a framework does not correspond to the reality because the majority of range sensors currently available on the market or even prototypes found in laboratories do not

Manuscript received May 26, 2002; revised June 18, 2003. This work was supported in part by the Natural Sciences and Engineering Research Council of Canada, in part by the Canadian Foundation for Innovation, and in part by the Ontario Innovation Trust.

The authors are with the Vision, Imaging, Video and Audio Research Laboratory, School of Information Technology and Engineering, University of Ottawa, Ottawa, ON, K1N 6N5 Canada (e-mail: ppayeur@site.uottawa.ca; chenadiu@site.uottawa.ca).

Digital Object Identifier 10.1109/TIM.2003.817910

provide such full images by themselves. They rather generate single points or scan lines of range measurements [18] or rely on an external mechanical device to translate the sensor or change its orientation [19].

In this paper, we introduce an approach to estimate registration between sensor viewpoints that makes use of a compact representation of raw data as they are provided by a single line laser range sensor. The compact mapping of surfaces eliminates the need for an exhaustive search for features [20]–[22] and the computation of sophisticated representations [16], [23]. The technique does not require any help from an external position/orientation tracking device to provide an initial estimate of the translation and rotation between successive viewpoints and no offline calibration is necessary. As a result, the computation of registration parameters from raw range data, independently from any positioning device, enhances the flexibility of sensing systems for a variety of applications. The following sections describe how scan lines are processed to create a compact representation of the surface shape. Estimation of the rotation and translation parameters is then detailed. Finally, experimental results using simulated and real range measurements are presented and discussed.

II. Proposed Approach

Most man-made objects are composed of a set of planar surfaces. Even objects of a higher complexity can be approximated by a set of planar surfaces that are easy to represent. Under the rigidity constraint, these planar regions remain unchanged no matter from which viewpoint they are observed. Only their projection on the image plane, and therefore their distance with respect to the range sensor are affected. As a consequence, only the relative position and orientation of the sensor has an influence on the object virtual representation. It is then possible to take advantage of these planar regions to estimate the registration between two or more sets of measurements gathered from different viewpoints. These assumptions are similar to those made in most research work on the problem of registration estimation. However, a majority of techniques invest a lot of efforts in building a sophisticated representation of object surfaces before they actually estimate the position and orientation parameters. Roth [16] provides a nice example of that by proposing a registration technique that is based on a match between surface representations obtained by means of a Delaunay triangulation. Even though this approach performs well, the conversion of raw range measurements into a triangular mesh mapping of the object surface is computationally expensive. As a result, much time is spent on modeling objects with respect to a camera-based reference frame while the actual goal is to estimate the motion of the sensor between viewpoints. The strategy that is presented here rather relies on basic planar patches surface representation. This way, the emphasis is put on the estimation of the sensor's position and orientation variations between viewpoints in 3-D space rather than on an intermediate modeling technique or feature extraction procedure.

A Jupiter laser range sensor based on an active optical triangulation technology developed at the National Research Council of Canada and commercialized by Servo-Robot, Inc. is used.

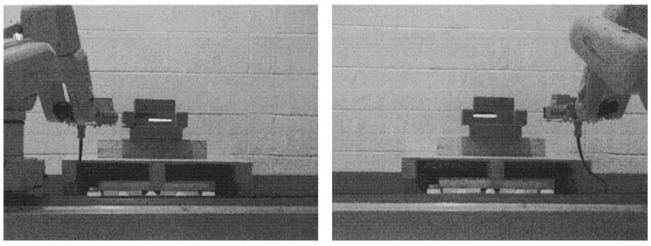

Fig. 1. Range sensor scanning from two different viewpoints.

This range finder provides a single scan line of up to 256 unevenly distributed range measurements with a resolution of up to 0.1 mm, a scan time of about 25 ms, and a maximum depth of one meter. In order to cover a significant surface of the scene, the sensor is moved with an approximately constant orientation along a vertical line to collect a series of scan profiles on the visible surface of the object. The small displacements between successive scan profiles are under the control of a CRS-F3 robotic arm on which the range sensor is mounted. The robot is operated in the world coordinates mode in order to ensure a precise control of the sensor position. Next, the sensor is moved to a completely different viewpoint and the process is repeated to collect a new set of profiles. Fig. 1 shows the experimental setup for two viewpoints.

Our goal is to estimate the rotations, R_{ij}, and the translations, T_{ij}, between two successive viewpoints from which range measurements have been collected as shown in Fig. 2. The first step consists in segmenting each range profile and in approximating them with local straight line segments. This allows to overcome the difficulties associated with the irregular spacing between points on the same scan profile that preempts a point-based matching between two profiles. Next, the neighbor profiles that show similar shapes are merged into planar patches of various sizes.

The respective normal vectors, areas and centroids of these patches are then computed and used to encode the surface representation as a modified Gauss sphere which significantly simplifies the search for rotation parameters. Indeed, provided two sets of scan profiles encoded as Gauss spheres, rotation parameters are estimated by finding the best rotation values that make corresponding normal vectors to overlap. As a final step, translation parameters relating the two sets of scan profiles, and therefore defining the displacement of the sensor between viewpoints, are estimated by computing the necessary shift of the patch centroids that make corresponding planar patches to match when the previously computed rotation transformation is applied to one set. Fig. 3 illustrates the data flow of the proposed approach. Details on each step are provided in the following section.

III. Compact Representation of Surfaces

The proposed approach relies on a simple planar approximation of surface shapes that is easily computed from raw range measurements to generate compact surface maps that can be matched to estimate the rotation and translation parameters between different viewpoints [24]. This section describes the two-step procedure that is used to obtain the modified Gauss sphere representation of surfaces.

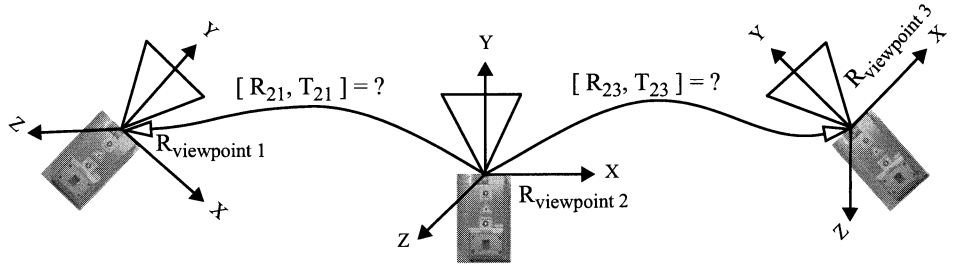

Fig. 2. Registration problem: estimating rotations and translations between viewpoints.

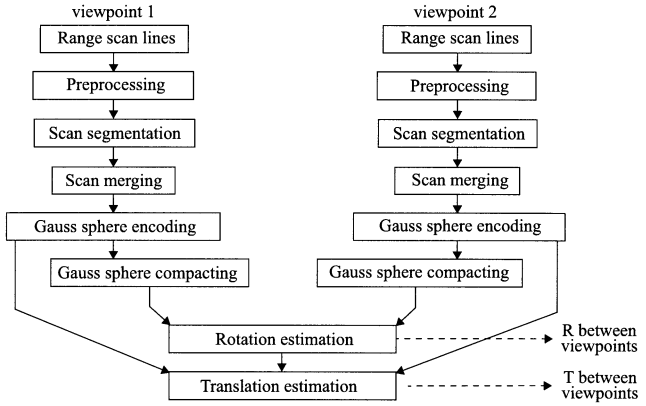

Fig. 3. Data processing for registration estimation.

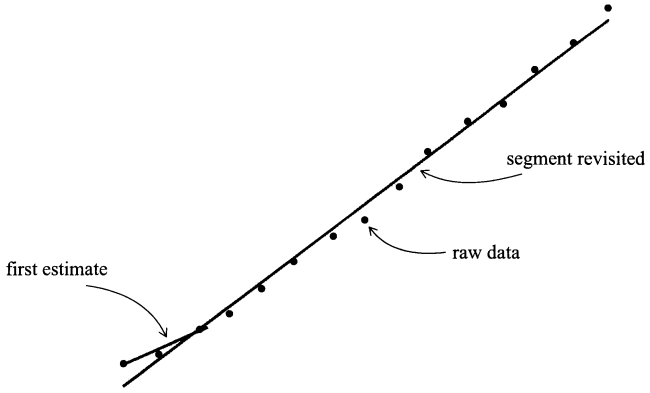

Fig. 4. Straight-line fitting on a sequence of range measurements.

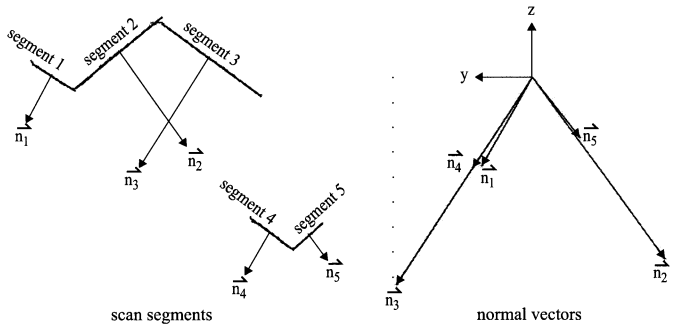

Fig. 5. Compact representation of a segmented range profile.

A. Segmentation of Range Profiles

Starting from the raw range measurements, a first preprocessing procedure is applied to remove outliers and to smooth the profile with a median filter that reduces the effects of noise. This eliminates large deviations that often occur in raw measurements. Next, a straight-line fitting technique is applied as shown in Fig. 4. The process starts at one extremity of the profile. Three measurements are initially used to determine the orientation of the straight line. The following points encountered along the profile are then successively checked for their proximity in terms of the distance with respect to the initial line estimate. When the deviation between a measurement point and the straight line estimate is below a given threshold (4 mm in our experiments), then the point is considered to be part of the current straight-line segment. A segment is terminated when the distance between a measurement point and the straight-line estimate is above the selected threshold. In this case, a new straight-line segment is initialized and the remaining points in the profile are successively checked for their proximity with this new segment following the same procedure. The process is repeated until the end of the profile is reached. Once a segment is terminated, its estimation is refined by recomputing the parameters of the segment on the basis of the entire set of measurement points that have been associated with it.

Normal vectors, lengths, and center points of each straight-line segment are computed to parameterize the representation of the profile and to obtain a compact mapping as shown in Fig. 5. The length of each segment defines the length of the corresponding normal vector. As a result, a scan profile of 256 measurements can be encoded as a set of $2a$ parameters, where a is the number of straight-line segments associated with the profile.

B. Scan Merging

The profile segmentation previously obtained provides an efficient way to merge similar neighboring range profiles and to create a patch-based surface representation. Assuming that the gap between two successive scan profiles collected from the same viewing area is kept small enough to ensure a proper coverage of the object surfaces (5 mm in our experiments), the variation of the shape between successive profiles should be smooth except on object edges. As a consequence, successive profiles should have a similar normal vector distribution where the object surfaces are continuous. The straight-line approximations of neighbor profiles obtained in the previous step are then compared to check for similarity. If the angle and the length of normal vectors associated with each straight-line segment are within a given deviation (0.025 radian for angle and 25% in

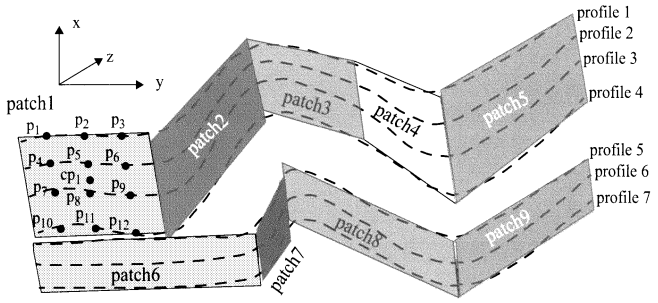

Fig. 6. Definition of patches as combined segmented profiles.

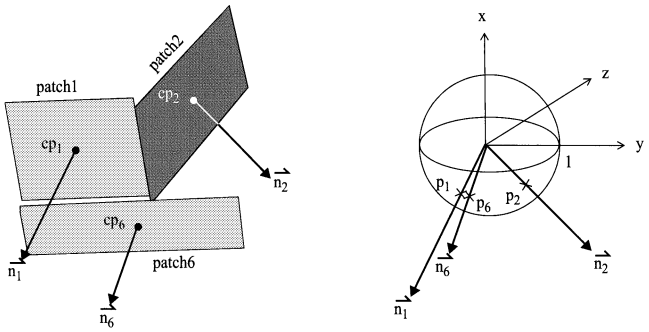

Fig. 7. Compact Gauss sphere representation of a surface shape.

length in our experiments), then neighbor profiles are considered similar and are combined to create one planar patch for each of their segments. For example in Fig. 6, profiles 1 to 4 have been collected on a continuous surface and can therefore by combined. As these profiles have been previously segmented, a different surface patch is created for each scan segment (patches 1 to 5 inclusively). The same idea applies to profiles 5, 6, and 7 as they are similar.

On the other hand, transitions between objects result in abrupt changes between two successive profiles. When such a transition occurs, the respective profiles are assigned to different patches This is the case of profiles 4 and 5 which are successive scan lines in the raw data set but are not similar. Locating this transition allows to delimitate the boundaries between planar patches associated with the first and the second group of profiles respectively.

This way, planar patches are defined for each group of combined straight-line segments. Three points from each segment are considered to estimate the patch orientation. Fig. 6 illustrates the process for the first patch as p_1, p_2, and p_3 are selected from the first segment in profile 1, while p_4, p_5, and p_6 are extracted from the corresponding segment in the second profile. Knowing the distance between two successive profiles from our acquisition setup, the X, Y coordinates of p_4 can be estimated. The corresponding Z coordinate of p_4 is then extracted from the first segment of the second profile. The same steps also apply to estimate p_5 and p_6 coordinates. Eventually, the process is repeated to locate p_7 to p_9 from p_4 to p_6 and so on for as many profiles as necessary to fully define a given planar patch.

For each planar patch previously defined, the center point coordinates, cp_i, the normal vector, $\vec{n}_i$, and the area are computed to define the best fitting planar surface parameters. The center point is defined as the average of the coordinates of the N points, p_i, associated with the patch

$$cp_i = \frac{1}{N}\sum_{i=1}^{N} p_i. \tag{1}$$

The normal vector, $\vec{n}_i$, corresponds to the smallest eigen vector of the matrix $\alpha^T\alpha$, where:

$$\alpha = \begin{bmatrix} x_1 & y_1 & z_1 & 1 \\ x_2 & y_2 & z_2 & 1 \\ \dots & \dots & \dots & 1 \\ x_N & y_N & z_N & 1 \end{bmatrix} \tag{2}$$

with $p_i = (x_i, y_i, z_i)$. The length of this normal vector is set equal to the area of the planar patch.

The vector representation used for line segments is now extended to 3-D space under the form of a modified Gauss sphere representation to create a compact encoding of the distribution of patches that describe the surfaces as shown in Fig. 7. But given the relatively large number of planar patches that might exist in a real 3-D scene, we observed that this representation can still be advantageously compacted to a limited number of normal vectors. Specifically, those normal vectors which differ by a small angular difference can advantageously be merged into a single vector with their respective lengths added. Merging these vectors is equivalent to the unification of patches that have a very similar orientation (within some tolerance level) with no consideration of their respective depth with respect to the sensor or their position in the field of view. Fig. 7 shows the metric of co-normality that we introduced to select normal vectors that can be merged. $\vec{n}_1$ and $\vec{n}_6$ are two normal vectors corresponding to two planar patches. p_1 and p_6 are their projection points on the unit sphere surface. If the Euclidean distance between p_1 and p_6 is less than a given threshold (0.14 mm in our experiments), then $\vec{n}_1$ and $\vec{n}_6$ can be merged. The resulting vector $\vec{n}$ has a total length of $|\vec{n}_1| + |\vec{n}_6|$. In practice, the number of normal vectors is significantly reduced by this process. This opportunity to further reduce the complexity of the representation is provided by the fact that most objects can be approximated by a large number of separated patches, many of them having a similar orientation.

In comparison with the thousands of 3-D points collected by the range sensor, this simplified representation is much more compact. As a consequence, processing time for the registration parameters estimation is significantly shortened as the matching between representations from each viewpoint is simplified. In spite of some lost in the resolution of the representation, this strategy proves to be sufficiently accurate for many robotic applications while it significantly speeds up the computation in comparison with classical triangular mesh solutions that are more dedicated to rendering applications.

IV. Registration Estimation

Starting from the compact Gauss sphere representation, three rotation parameters between successive viewpoints can be directly estimated from the set of normal vectors, $\vec{n}_i$. Next, three translation parameters can be computed from the center points coordinates of planar patches, cp_i, while taking into account the rotation values previously obtained.

A. Rotation Parameters Estimation

Three correspondences of normal vectors are required to uniquely determine the rotation matrix, R, from which three rotation angles, (θ, φ, ψ), can be computed [25]. Provided that $\vec{n}_1$ and $\vec{n}'_1$, $\vec{n}_2$ and $\vec{n}'_2$, and $\vec{n}_3$ and $\vec{n}'_3$ are three nondegenerated sets of corresponding normal vectors respectively extracted from the two sets of raw data associated with two viewpoints between which a rotation, R, has been applied, these vectors must satisfy the following constraint equations:

$$\vec{n}_1 = R\,\vec{n}'_1 \tag{3}$$
$$\vec{n}_2 = R\,\vec{n}'_2 \tag{4}$$
$$\vec{n}_3 = R\,\vec{n}'_3 \tag{5}$$

if we let

$$\vec{n}_1 = [x_1, y_1, z_1] \quad \text{and} \quad \vec{n}'_1 = [a_1, b_1, c_1] \tag{6}$$
$$\vec{n}_2 = [x_2, y_2, z_2] \quad \text{and} \quad \vec{n}'_2 = [a_2, b_2, c_2] \tag{7}$$
$$\vec{n}_3 = [x_3, y_3, z_3] \quad \text{and} \quad \vec{n}'_3 = [a_3, b_3, c_3] \tag{8}$$

and the rotation matrix

$$R = \begin{bmatrix} g & h & i \\ j & k & l \\ m & p & q \end{bmatrix}. \tag{9}$$

The values of the rotation matrix parameters can be computed by solving the following system of equations for the rightmost vector

$$\begin{bmatrix} x_1 \\ y_1 \\ z_1 \\ x_2 \\ y_2 \\ z_2 \\ x_3 \\ y_3 \\ z_3 \end{bmatrix} = \begin{bmatrix} a_1 & b_1 & c_1 & 0 & 0 & 0 & 0 & 0 & 0 \\ 0 & 0 & 0 & a_1 & b_1 & c_1 & 0 & 0 & 0 \\ 0 & 0 & 0 & 0 & 0 & 0 & a_1 & b_1 & c_1 \\ a_2 & b_2 & c_2 & 0 & 0 & 0 & 0 & 0 & 0 \\ 0 & 0 & 0 & a_2 & b_2 & c_2 & 0 & 0 & 0 \\ 0 & 0 & 0 & 0 & 0 & 0 & a_2 & b_2 & c_2 \\ a_3 & b_3 & c_3 & 0 & 0 & 0 & 0 & 0 & 0 \\ 0 & 0 & 0 & a_3 & b_3 & c_3 & 0 & 0 & 0 \\ 0 & 0 & 0 & 0 & 0 & 0 & a_3 & b_3 & c_3 \end{bmatrix} \begin{bmatrix} g \\ h \\ i \\ j \\ k \\ l \\ m \\ p \\ q \end{bmatrix}. \tag{10}$$

The resulting rotation matrix is then checked for orthogonality before the three rotation angles are extracted. For a rotation matrix, R, defined in accordance with the standard roll-pitch-yaw (RPY) convention [26], these rotation angles, (θ, φ, ψ), can be extracted as follows:

$$\theta = \operatorname{atan}(j, g) \tag{11}$$
$$\varphi = \operatorname{atan}(-m, j\sin\theta + g\cos\theta) \tag{12}$$
$$\psi = \operatorname{atan}(p, q) \tag{13}$$

where θ represents the rotation around the Z axis, φ is the rotation around the Y axis, and ψ is the rotation around the X axis of the reference frame.

Applying the computed rotation matrix to all normal vectors in one of the Gauss sphere representations should result in the overlap of some of these vectors with those of the compact mapping associated with the other viewpoint. However, because of errors in the measurements and the approximations made on the surface representation, the matching might not be exact. In order to refine the estimation of the rotation matrix, its computation is repeated for all possible triplets of matching normal vectors in the simplified Gauss sphere representation. The rotation parameters that lead to a maximum overlap (in terms of length) between normal vectors are considered to be the best estimate for the rotation matrix.

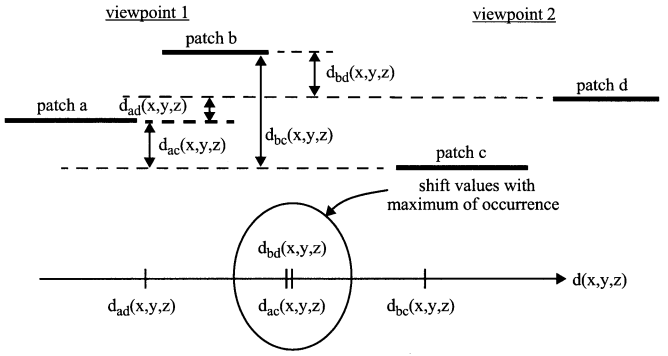

Fig. 8. Occurrence of shift values between matching patches.

B. Translation Parameters Estimation

Once the rotation parameters have been estimated, the application of the resulting rotation matrix to one Gauss sphere representation leads to two sets of normal vectors having the same orientation but submitted to a shift in 3-D space. Therefore, the translation parameters, $T = [dx, dy, dz]$, can be estimated as the required translations along the reference axes between the centroids associated with each surface patch. Mathematically, this can be formulated as follows: if a normal vector, $\vec{n}$, and a centroid point, cp, refer to one patch while $\vec{n}'$ and cp' refer to another patch, and $\vec{n}$ matches $\vec{n}'$ when the rotation matrix is applied on the second patch, then we have

$$\begin{bmatrix} cp \\ 1 \end{bmatrix} = \begin{bmatrix} R & T \\ 0 & 1 \end{bmatrix} \begin{bmatrix} cp' \\ 1 \end{bmatrix} \tag{14}$$

where R is the rotation matrix previously estimated. Placing T in evidence leads to

$$T = cp - R \cdot cp'. \tag{15}$$

As many surface patches need to be matched, a good estimate of the translation parameters is the average of the necessary displacement along each axis over all matched centroids, that is

$$T = \frac{1}{N}\sum_{i=1}^{N}(cp_i - R \cdot cp'_i) \tag{16}$$

where N is the number of correspondences between centroid points.

The matched centroids correspond to patches having similar orientation. However, as many patches in the surface description might share the same orientation, this tends to result in some false matches of centroids. But statistically, the correct translation parameter set can be defined as the one with the maximum number of correspondences when all possible matching possibilities are considered between pairs of patches. Fig. 8 illustrates this idea with two pairs of patches respectively seen from the first and the second viewpoint.

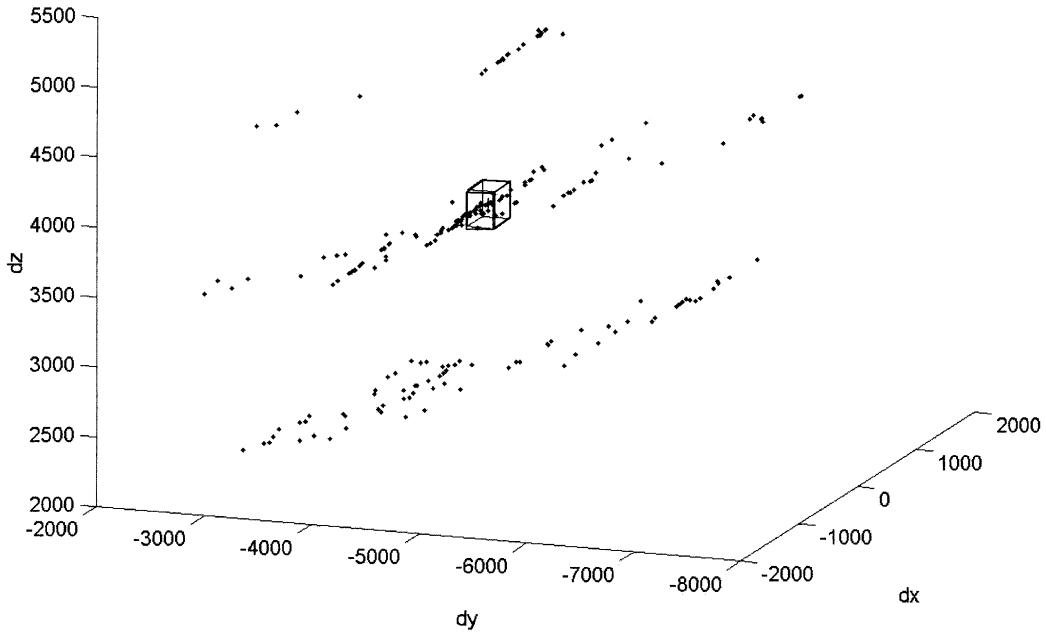

Fig. 9. Experimental graph of shifts occurrence.

Here the computed rotation matrix has already been applied to the second set of patches in order to realign it with the first one. Considering all possible shifts in this simple case, four pairs of matching patches are obtained with their respective translation values being: $d_{ac}(x,y,z)$, $d_{ad}(x,y,z)$, $d_{bc}(x,y,z)$, and $d_{bd}(x,y,z)$. However, only $d_{ac}(x,y,z)$ and $d_{bd}(x,y,z)$ are appropriate estimates as they correspond to a correct shift for each of the patches from the first and second viewpoints. A graph of shifts occurrence then allows to easily determine those shift values that lead to a maximum correspondence between planar patches. Fig. 9 shows a graph of shifts occurrence computed from experimental data. Each possible shift is represented as a 3-D point. These translation coordinate points tend to spread everywhere in the graph space. But the area with the highest density of points along each axis, that is depicted by the small cube, corresponds to the maximum of occurrence of some shifting values that lead to a good estimate of the actual translation parameters. A weighted average of those shifting values contained in the maximum of occurrence region is computed along each axis to provide an estimate for $T = [dx, dy, dz]$.

V. Experimental Results

The proposed algorithm has been tested on the experimental testbed shown in Fig. 1. The development and validation of the algorithm has been made on a set of range profiles collected on various objects with a Jupiter range finder mounted on a 7-DOFs robotic arm. However, the robotic arm is only used to move the sensor and to validate the results. Fig. 10 shows a set of 44 profiles of range measurements collected from the right-side viewpoint in the setup of Fig. 1 and the corresponding patch representation. The results of the registration estimation procedure are illustrated in Fig. 11 as a fitted superposition between the left and the right sets of raw range measurements. We observe that the alignment between the measurements along all axes is very good both in translation and in rotation. This demonstrates that registration parameters can be accurately estimated in spite of the simplicity of the surface representation.

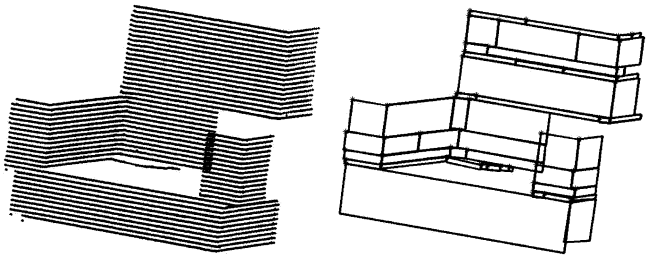

Fig. 10. Range measurements from the right viewpoint and corresponding patch representation.

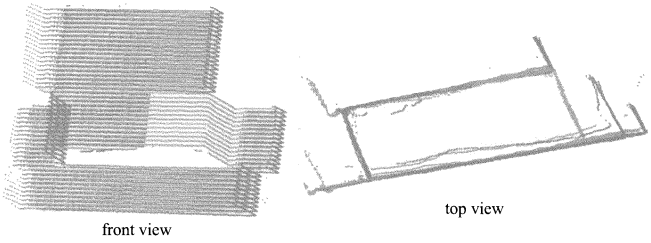

Fig. 11. Superposition of two sets of scan lines after registration.

Fig. 12 presents experimental results on a more complex scene composed of a standard computer setup which has been scanned from three different viewpoints. 40 range profiles containing 256 points each are collected from each viewpoint to fully cover the scene area. Estimating registration parameters with the proposed technique and applying the resulting transformation matrices to the raw data sets leads to a very good superposition of corresponding surfaces as shown in Fig. 13 for a front and a top view projections. In both cases, we observe that the orientation and the translation between viewpoints have been compensated such that the shape of the objects shown

TABLE I
COMPARISON OF REGISTRATION PARAMETERS BETWEEN THREE VIEWPOINTS FOR THE COMPUTER SETUP

Transformation parameters	center to left viewpoint		center to right viewpoint		left to right viewpoint	
	Theoretical	Experimental	Theoretical	Experimental	Theoretical	Experimental
Rotation (X)	0^o	-0.05^o	0^o	-0.07^o	2.67^o	2.77^o
Rotation (Y)	5.15^o	5.04^o	-5.15^o	-4.93^o	-9.95^o	-9.66^o
Rotation (Z)	14.89^o	14.96^o	-14.89^o	-14.64^o	-30.01^o	-29.46^o
Translation (X)	0 mm	-1.3 mm	0 mm	0.08 mm	0 mm	12.6 mm
Translation (Y)	300 mm	313 mm	-260 mm	-256 mm	-541.3 mm	-572.3 mm
Translation (Z)	0 mm	6.7 mm	0 mm	0.16 mm	143.8 mm	142.5 mm

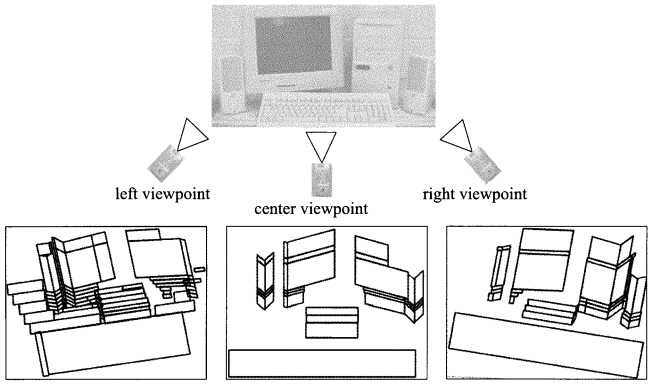

Fig. 12. Compact surface representation of a computer setup.

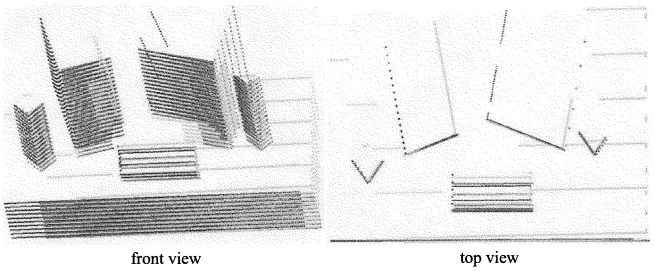

Fig. 13. Superposition of three sets of scan lines after registration for the computer setup.

in Fig. 12 can be easily recognized. A numerical comparison between theoretical and experimental data is presented in Table I.

Experimental results demonstrate that the proposed approach provides registration parameter estimates that are sufficiently accurate for many applications such as space modeling for path planning and collision avoidance in robotics [27] and eventually for virtual representation of artifacts at a medium-low resolution.

We notice that the error level on translation estimates is somewhat higher than on rotation. This fact is due to the difficulty to determine the best size for the region of maximum of occurrence in the graph that is used to extract translation values. Also, the precision of the estimates appears to be influenced by the distance between viewpoints. This is justified by a lower level of overlap between matching surfaces that occur when only the leftmost and the rightmost viewpoints are considered to estimate registration parameters.

Our experiments revealed that for geometrically symmetric objects having only a few distinctive surfaces, an overlap of up to 50% between the scan areas might be required to achieve correct registration. For usual man-made objects, the required overlap area is much less. However, the required degree of overlap directly depends on the complexity of objects contained in the scene. Increasing the overlap between scan areas increases the reliability and the accuracy of registration parameter estimates but makes the scanning process longer.

The proposed approach is also promising in terms of performance. The algorithm has been implemented on Matlab running on a Pentium III-933 Mhz with 256 MB RAM. The processing time required to estimate one set of registration parameters on the computer setup example is about 6 seconds including the construction of the compact representation of surfaces. This corresponds to about 150 ms per pair of scan lines to be registered. Experiments also demonstrated that the processing time can been reduced by a factor of 6 to 10 with an optimized implementation of the proposed technique in C running on the same computer.

Overall, the scan segmentation and the surface representation as a compact modified Gauss sphere reveal to significantly improve computation efficiency while not significantly degrading the accuracy of registration parameter estimates. This strategy also makes patch fitting simpler and faster. Using the overlap between normal vectors as an evaluation factor rather than the number of matched points between the two sets of data also speeds up computation. Moreover, this approach uses more points to estimate the surface patches than triangular meshes. This results in surface representations that are less sensitive to noise measurements.

VI. CONCLUSION

We have introduced an automatic approach for registration estimation based on raw range measurements provided by a single line laser range sensor. Registration parameters are efficiently computed without any need for an external device to provide an initial estimate. The approach does not require any human interaction and no sophisticated feature extraction or triangulation. Assuming only object rigidity and some overlap be-

tween the scanned areas, the approach allows to estimate the full set of six rotation and translation parameters that link 3-D scans gathered from different viewpoints. Taking advantage of a modified Gauss sphere representation, the mapping of planar patches that result from the merge of similar range profiles is significantly compacted. This solution results in an important reduction of the computational workload while providing efficient means for viewpoints matching estimation and validation all along the process. The proposed approach provided excellent experimental results both on simulated data and on profiles collected with a Jupiter range finder. The accuracy of the estimated registration parameters is sufficient for most applications in robot navigation with collision avoidance where computing time is a critical issue that makes more sophisticated algorithms based on triangular meshes or high-level feature extraction not tractable. An implementation in C demonstrated that this technique can be tractable for online operating systems.

Further developments to this registration technique will examine some alternative ways to merge range profiles in the areas where only a small number of scan lines exhibit similar characteristics. Some improvements in the planar patch estimation module might also be introduced to deal with generic objects that could advantageously be represented by nonrectangular patches. Finally, enhancements on the determination of maximum occurrence of shifting values could improve the translation parameters accuracy.

REFERENCES

[1] J. R. Miller, O. Amidi, and M. Delonis, "Arctic test flights of the CMU autonomous helicopter," in *Proc. 26th Annu. Symp. Association for Unmanned Vehicle Systems*, July 1999.

[2] L. P. Normand, "Sonar-Based Real World Mapping System," Master Degree thesis, School of Information Technology and Engineering, University of Ottawa, Ottawa, ON, Canada, 1990.

[3] M. K. Reed and P. K. Allen, "3-D modeling from range imagery: an incremental method with a planning component," *Image Vis. Comput.*, vol. 17, pp. 99–111, 1999.

[4] F. Lu and E. Milios, "Globally consistent range scan alignment for environment mapping," *Auton. Robots*, vol. 4, no. 4, pp. 333–349, Oct. 1997.

[5] V. Sequeira, K. Ng, E. Wolfart, J. G. M. Goncalves, and D. C. Hogg, "Automated 3-D reconstruction of interiors with multiple scan-views," in *Proc. SPIE Videometrics VI*, vol. 3641, Jan 1999, pp. 106–117.

[6] P. Besl and N. McKay, "A method for registration of 3-D shapes," *IEEE Trans. Pattern Anal. Mach. Intell.*, vol. 14, pp. 239–256, Feb. 1992.

[7] Y. Chen and G. Medioni, "Object modeling by registration of multiple range images," *Image Vis. Comput.*, vol. 10, no. 3, pp. 145–155, 1992.

[8] T. Masuda and N. Yokoya, "A robust method for registration and segmentation of multiple range images," *Computer Vis. Image Understanding*, vol. 61, no. 3, pp. 295–307, 1995.

[9] C. Dorai, G. Wang, A. K. Jain, and C. Mercer, "Registration and integration of multiple object views for 3-D model construction," *IEEE Trans. Pattern Anal. Mach. Intell.*, vol. 20, pp. 83–89, Jan. 1998.

[10] C.-S. Chen, Y.-P. Hung, and J.-B. Cheng, "RANSAC-based DARCES: a new approach to fast automatic registration of partially overlapping range images," *IEEE Trans. Pattern Anal. Mach. Intell.*, vol. 21, pp. 1229–1234, Nov. 1999.

[11] R. Bergevin, D. Laurendeau, and D. Poussart, "Registering range views of multipart objects," *Comput. Vis. Image Understanding*, vol. 61, no. 1, pp. 1–16, 1995.

[12] C. S. Chua and R. Jarris, "3-D free-form surface registration and object recognition," *Int. J. Comput. Vis.*, vol. 17, no. 1, pp. 77–99, 1996.

[13] D. F. Huber, "Automatic 3-D modeling using range images obtained from unknown viewpoints," in *Proc. IEEE Int. Conf. 3-D Digital Imaging and Modeling*, May 2001, pp. 153–160.

[14] C. Dorai, J. Weng, and A. K. Jain, "Optimal registration of object views using range data," *IEEE Trans. Pattern Anal. Mach. Intell.*, vol. 19, pp. 1131–1138, Oct. 1997.

[15] M. D. Elstrom and P. W. Smith, "Stereo-based registration of multisensor imagery for enhanced visualization of remote environments," in *Proc. IEEE Int. Conf. Robotics and Automation*, vol. 3, May 1999, pp. 1948–1953.

[16] G. Roth, "Registering two overlapping range images," in *Proc. 2nd Int. Conf. 3-D Digital Imaging and Modeling*, Ottawa, Canada, 1999, pp. 191–200.

[17] R. Szeliski, "Estimating motion from sparse range data without correspondence," in *Proc. Int. Conf. Computer Vision*, vol. 88, Dec. 1988, pp. 207–216.

[18] S. F. El-Hakim, J.-A. Beraldin, G. Godin, and P. Boulanger, "Two 3-D sensors for environment modeling and virtual reality: calibration and multi-view registration," in *Int. Archives Photogramm. Remote Sens.*, vol. 31, Vienna, 1996, pp. 140–146.

[19] D. Laurendeau, C. Gosselin, F. Caron, S. Comtois, T. Laliberté, and F. Loranger, "A random access 3-D/2D vision sensor," in *Proc. Vision Interface*, Vancouver, BC, Canada, June 1998, pp. 93–100.

[20] P. Neugebauer, "Geometrical cloning of 3-D objects via simultaneous registration of multiple range images," in *Proc. Int. Conf. Shape Modeling Applicat.*, Mar. 1997, pp. 130–139.

[21] N. Kehtarnavaz and S. Mohan, "A frame work for estimation of motion parameters from range images," *Comput. Vis., Graphics Image Processing*, vol. 45, no. 1, pp. 88–105, 1989.

[22] C.-S. Chen, Y.-P. Hung, and J.-B. Cheng, "A fast automatic method for registration of partially overlapping range images," in *Proceedings of the International Conference on Computer Vision*, 1998, pp. 242–248.

[23] G. Turk and M. Levoy, "Zippered polygon meshes from range images," in *Proc. SIGGRAPH*, 1994, pp. 311–318.

[24] C. Chen, "Registration of Range Measurements With Compact Surface Representation," Master Degree thesis, School of Information Technology and Engineering, University of Ottawa, Ottawa, ON, Canada, Sept. 2002.

[25] E. Trucco and A. Verri, *Introductory Techniques for 3-D Computer Vision*. Englewood-Cliffs, NJ: Prentice-Hall, 1998.

[26] J. J. Craig, *Introduction to Robotics, Mechanics and Control*, 2nd ed. Reading, MA: Addison-Wesley, 1995.

[27] P. Payeur, C. M. Gosselin, and D. Laurendeau, "Range data merging for probabilistic octree modeling of 3-D workspaces," in *Proc. IEEE Int. Conf. Robotics and Automation*, vol. 4, May 1998, pp. 3071–3078.

Pierre Payeur (S'90–M'98) received the Ph.D. degree in electrical engineering from Laval University, Quebec City, QC, Canada, in 1999 with a thesis on probabilistic octree modeling for telerobotic applications.

From 1991 to 1998, he was a Research Assistant and a Lecturer at Laval University in the field of industrial process control. In 1998, he joined the University of Ottawa, Ottawa, ON, Canada, as an Assistant Professor in the School of Information Technology and Engineering (SITE) where he cofounded the Vision, Imaging, Video, and Audio Research Laboratory (VIVA). His current research interests are volumetric 3-D modeling, range data processing, robot guidance, teleoperation, and integration of computer vision in autonomous systems control.

Dr. Payeur is a member of the Ordre des Ingénieurs du Québec.

Changzhong Chen received the B.S. and M.Sc.A. degrees in electrical engineering from Xiamen University, China, and from the University of Ottawa, Ottawa, ON, Canada, respectively, in 1998 and 2002, respectively. He is currently pursuing the Ph.D. degree in electronics at Carleton University, Ottawa.

His research interests include modeling and simulation of high-speed interconnects, computer-aided design of VLSI circuits and systems, numerical algorithms, computer vision, 3-D modeling, and medical image processing.